IRIS AperTO

UNIVERSITÀ DEGLI STUDI DI TORINO

AperTO - Archivio Istituzionale Open Access dell'Università di Torino

Simulating the effects of wet and dry on aggregate dynamics in argillic fragipan horizon

This is the author's manuscript

Original Citation:

Availability:

This version is available http://hdl.handle.net/2318/1644875 since 2017-07-11T12:39:57Z

Published version:

DOI:10.1016/j.geoderma.2017.06.026

Terms of use:

Open Access

Anyone can freely access the full text of works made available as "Open Access". Works made available under a Creative Commons license can be used according to the terms and conditions of said license. Use of all other works requires consent of the right holder (author or publisher) if not exempted from copyright protection by the applicable law.

(Article begins on next page)

05 November 2024

IRIS AperTO

UNIVERSITÀ DEGLI STUDI DI TORINO

This Accepted Author Manuscript (AAM) is copyrighted and published by Elsevier. It is posted here by agreement between Elsevier and the University of Turin. Changes resulting from the publishing process - such as editing, corrections, structural formatting, and other quality control mechanisms - may not be reflected in this version of the text. The definitive version of the text was subsequently published in GEODERMA, 305, 2017, 10.1016/j.geoderma.2017.06.026.

You may download, copy and otherwise use the AAM for non-commercial purposes provided that your license is limited by the following restrictions:

(1) You may use this AAM for non-commercial purposes only under the terms of the CC-BY-NC-ND license.

(2) The integrity of the work and identification of the author, copyright owner, and publisher must be preserved in any copy.

(3) You must attribute this AAM in the following format: Creative Commons BY-NC-ND license (http://creativecommons.org/licenses/by-nc-nd/4.0/deed.en), 10.1016/j.geoderma.2017.06.026

The publisher's version is available at:
http://linkinghub.elsevier.com/retrieve/pii/S0016706117301064

When citing, please refer to the published version.

Link to this full text:
http://hdl.handle.net/2318/1644875

This full text was downloaded from iris - AperTO: https://iris.unito.it/

iris - AperTO

University of Turin's Institutional Research Information System and Open Access Institutional Repository

Title

Effects of wet and dry on aggregate dynamics in fragipan: an experimental approach

Authors

Gloria Falsone[a], Silvia Stanchi[b,c], Eleonora Bonifacio[b]

[a]DIPSA – Alma Mater Studiorum University of Bologna, via Fanin 40, 40127 Bologna, Italy

[b]DISAFA, University of Torino, Largo P. Braccini 2, 10095 Grugliasco, TO, Italy

[c]NATRISK, Research Centre on Natural Risks in Mountain and Hilly Environments, University of Torino, Largo P. Braccini 2, 10095 Grugliasco, TO, Italy

Corresponding author

Gloria Falsone: tel +39 051 209 6229, Email gloria.falsone@unibo.it

Abstract

Fragipan is a dense and usually brittle subsurface soil horizon, limiting the penetration of roots and the infiltration of water. Genesis of fragipan is still unclear; however there is a general agreement on the importance of wet-dry cycles in its evolution. Furthermore, in addition to the effect of

water, in argillic Bx horizon, the presence of cations affecting the clay dispersion/flocculation behaviour might be a key factor in fragipan dynamics. In order to gain knowledge on the specific effect of alternating moisture conditions on the evolution of aggregates collected from Btx horizon, we evaluated the variations of physical properties caused by a wet-dry cycle using both deionized and Ca-enriched water on the 1-2 mm aggregate, and on newly formed aggregates (i.e. 2-5 and >5 mm size classes) obtained after a lab experiment. The obtained results were compared with a Bt horizon that did not show fragipan properties. Btx and Bt samples were collected from a Typic Fragiudalf on fluvio-glacial terraces in NW Italy. The two horizons had comparable clay content (around 13%), and their mineralogical composition was dominated by hydroxy-interlayed vermiculite and smectite.

The fragipan 1-2 mm aggregates before the treatments had low clay dispersion ratio (11.5%), and typically low volume of macropores (74 $mm^3\ g^{-1}$), high volume of mesopores (111 $mm^{-3}\ g^{-1}$), high slaking (30.1%), close packing of coarse particles and open arrangement of fine particles (0.82 and 0.31, respectively). The water treatment promoted the enrichment in flocculated-clay in the new-aggregates, and Ca-treatment enhanced clay flocculation both in the newly formed and in the 1-2 mm aggregates. The clay flocculation induced a denser arrangement of clay particles ($\geq$0.44), and a consequent reduction of mesopores (from 56.2 to 66.1 $mm^{-3}\ g^{-1}$), combined with the opening of the coarser particles packing ($\leq$0.78). This new particle arrangement did not correspond to the specific combination of coarse/fine particles arrangement of fragipan. The relative percentage of slaking also decreased. Therefore, upon both deionized water and $CaCl_2$ wetting and drying, the aggregates from fragipan changed and the specific physical properties of fragipan, measureable in laboratory, tended to be attenuated.

Highlights

- In fragipan, physical properties changes induced by wetting/drying are studied in the lab

– Water and $CaCl_2$ wetting/drying promoted the enrichment in flocculated-clay

- Flocculation induced a denser arrangement of clay particles and mesopores reduction

- The new arrangement did not correspond to the specific fragipan particle arrangement

- Water and $CaCl_2$ wetting/drying attenuated the fragipan physical characteristics measurable in laboratory

Keywords

Argillic horizons, clay dispersion/flocculation, BET, Hg porosimetry, wet aggregate stability

1. Introduction

Fragipan is a subsurface soil horizon limiting the penetration of roots and infiltration of water because of its high bulk density, low porosity, and discontinuous void space (Soil Survey Staff, 2014). The occurrence of fragipan (Bx horizons) in a soil profile can strongly reduce soil physical quality and functionality. No specific analytical determinations are however required for fragipan recognition, i.e. the fragic properties are identified in the field (Soil Survey Staff, 2014). Fragipan shows a hard or very hard consistence when dry, but it is brittle when moist, and its air-dried clods undergo immediate slaking once immersed in water (e.g., Bockheim and Hartemink, 2013; Lindbo et al., 1994). Falsone and Bonifacio (2009) demonstrated that the low permeability and high bulk density of fragipan result from a specific arrangement of mineral particles that is not found in any other soil horizons, i.e. an open packing of the clay phase is associated to an extremely dense packing of silt and sand.

Fragipan horizons occur in all parts of the world and are common in North-American Alfisols (Bockheim and Hartemink, 2013), in Luvisols and Albeluvisols in Ukraine (Nikorych et al. 2014), in Udalfs in Northern Italy (Falsone and Bonifacio, 2006; Ajmone-Marsan et al., 1994). In these environments they typically occur within an argillic (argic) horizon (Btx). Bockheim and Hartemink (2013) reviewed the descriptive models for the genesis of fragipan, and subdivided them based on the approach used. The physical models emphasized either the role that lithologic discontinuities or pore size distribution have on water flow and material accumulation into the fragipan, or the hydrocollapse of soil or parent material that can form hard pans. The chemical models, on the other hand, point to the importance of water translocated weathering products such as clay and Fe, Al, Si phases, as bonding agents and bridges of coarser particles. Wet-dry cycles have been indicated as one of the driving factors for fragipan evolution (e.g., Wilson et al., 2010; Boulet et al., 1998; Bruckert and Bekkary, 1992), but the role of alternating moisture conditions is still not well-understood, and contrasting results have been reported. Szymański et al. (2011) and Nikorych et al. (2014) stated that the seasonal soil wetting and

drying cause fragipan degradation through the formation of vertical cracks. Weisenborn and Schaetzl (2005a) reported that, upon wetting, argillic fragipans can degrade because of clay and Fe leaching due to vertically percolating water, thus developing non-brittle E horizon features. Attou and Bruand (1998) found instead that fragipan originates from successive wetting and drying cycles, because of the effect that alternating water conditions have on clay; wetting favours clay dispersion within the soil matrix and the subsequent dry period allows the reorganization of clay particles into coatings and bridges over and between the skeleton grains. In addition to the effect of water, in argillic Bx horizon, the presence of cations affecting the clay dispersion/flocculation behaviour should be therefore a key factor in fragipan dynamics.

This paper aims at understanding the role of wet-dry cycles on aggregates dynamics in Btx horizon, hypothesizing that the wet-dry cycle and the presence of flocculating cation, such as calcium, should differently affect the Bx physical properties. In laboratory conditions, the presence of calcium would favour clay flocculation enhancing the Bx properties both in pre-existing and newly-formed soil aggregates. To obtain a deeper insight into the mechanisms occurring upon wetting and drying in argillic fragipan we performed a laboratory experiment to evaluate the changes in those physical properties that are controlled by clay flocculation/dispersion behaviour and interactions between particles. The specific goals were: (i) to study the evolution of aggregates from a Btx horizon during a laboratory controlled wet-dry cycle, using both deionized water and a solution containing calcium (i.e., $CaCl_2$); (ii) to investigate the physical properties of newly-formed aggregates obtained from the Btx horizon upon wet-dry cycle in the laboratory. The results were compared to those of the upper Bt horizon (i.e. non-fragipan argillic).

.

2. Materials and Methods

77 *2.1. The study area*

78 In the catchment of the Stura di Lanzo River (45° 13.366’ N, 7° 31.399’ E), NW Italy, a fine-loamy mixed Typic Fragiudalf (Soil Survey Staff,
79 2014) was selected for this study. It develops on fluvio-glacial terraces of the Fiano Unit (Middle Pleistocene, i.e. Mindel-Riss interglacial in the
80 Alps) according to Forno et al. (2007). The dominant lithologies of the area eroded by the Pleistocene glacier are prasinites, serpentinites,
81 lherzolites, amphibolites, micaceous and chlorite schists, eclogites, and gneiss. The vegetation is dominated by *Robinia pseudoacacia* L. and
82 *Corylus avellana* L. The morphological description of a representative soil profile of the area is reported in Table 1. At the sampling site, the
83 fragipan horizon was identified at 165-190 cm depth by brittleness and morphology, including vertical seams, coarse prismatic structure, and
84 absence of roots in prisms (Soil Survey Staff, 2014).

85 Samples (~1 kg) of the argillic fragipan (Btcx) and the overlying argillic non-fragipan (Btc2) horizons were collected, air-dried and sieved to pass a
86 2-mm screen. The main properties of the <2 mm fraction of Btc2 and Btxc horizons are reported in Table 2. An aliquot of <2 mm air-dried of Btc2
87 and Btcx samples was further dry-sieved at 1 mm and the 1-2 mm aggregate class was separated.

88

89 *2.2. Sample preparation and treatment conditions*

90 One hundred grams of the <2 mm air-dried samples of each soil horizon were evenly distributed in a container and sprayed with 25 ml of deionized
91 water or 0.25M $CaCl_2$ (Figure 1). Four tests were thus performed: Btcx horizon plus deionized water, Btcx plus 0.25M $CaCl_2$, Btc2 horizon plus
92 deionized water, and Btc2 plus 0.25M $CaCl_2$. The samples were allowed to dry for 2 weeks at room temperature, ensuring the occurrence of both
93 new-aggregates formation and clay flocculation, i.e. the two main processes considered in this study. Both processes are in fact relatively rapid, and

94 in controlled conditions the formation of aggregates via particle interactions and/or clay flocculation can quickly occur (Fortun et al., 1989; Falsone
95 et al., 2007; Falsone et al. 2016). The experiment was replicated three times, originating therefore 12 samples. At the end of the treatment, the
96 samples were sequentially dry sieved on 5-, 2- and 1-mm sieves. Three fraction of aggregates were thus obtained: 1-2, 2-5 and >5 mm. The weight
97 of each aggregate class was recorded and the result was expressed as percentage. The >2 mm aggregate classes (i.e., 2-5 and >5 mm fractions) were
98 considered as newly formed aggregates (NEW-aggregates).
99 Three samples of 1-2 mm aggregates obtained by dry-sieving of <2 mm of Btc2 and Btcx samples were also put in the same laboratory conditions as
100 described above, but without any treatment.
101
102 The analyses were performed on the 1-2 mm aggregates without any treatment (FRG and NFRG), on the 1-2 mm aggregate fraction after the
103 treatment (FRG-WAT, FRG-CA, NFRG-WAT and NFRG-CA), and on the 2-5 (FRG_{2-5}-WAT, FRG_{2-5}-CA, $NFRG_{2-5}$-WAT and $NFRG_{2-5}$-CA) and
104 >5 mm NEW-aggregates (FRG_5-WAT, FRG_5-CA, $NFRG_5$-WAT and $NFRG_5$-CA).
105
106 *2.3. Chemical and physical analyses*
107 The organic carbon was measured by dry combustion (CE Instruments NA2100 elemental analyser, Rodano, Italy). The contents of pedogenic iron
108 oxides (FeDCB) were estimated through extraction with Na-dithionite-citrate-bicarbonate (Mehra and Jackson, 1960) and subsequent determination
109 of Fe by AAS (Perkin Elmer Analyst 400, Waltham, USA). The particle size distribution (PSD) was determined by the pipette method (Gee and
110 Bauder, 1986) after: (i) dispersion with deionized water only; (ii) dispersion with $(NaPO_3)_6$; (iii) dispersion with $(NaPO_3)_6$ after H_2O_2 oxidation of

111 organic matter and Na-dithionite-citrate-bicarbonate removal of Fe-cements. The PSD data were used to calculate the clay dispersion ratio (CDR)
112 according to Dong et al. (1983) as follows:

113 $$CDR = \frac{Clay\ obtained\ with\ deionized\ water}{Clay\ obtained\ with\ (NaPO_3)_6} \cdot 100 \quad (1)$$

114 The wet aggregate stability (WAS) was evaluated after 10 min in rotating 0.2-mm sieves (Kemper and Rosenau, 1986). The material remaining on
115 the sieves was then dried and weighed. Then, the amount of stable aggregates (>0.2 mm) was corrected for the content of coarse sand determined
116 after H_2O_2 oxidation and Na-dithionite-citrate-bicarbonate extraction. The WAS index was calculated as follows:

117 $$WAS = \frac{weight\ retained - weight\ of\ coarse\ sand}{total\ sample\ weight - weight\ of\ coarse\ sand} \cdot 100 \quad (2)$$

118 And the percentage of aggregate loss (Loss) as

119 $$Loss = 100 - WAS \quad (3)$$

120 To test the wet cohesion independently from slaking, thus regardless of the ruptures due to water saturation, 10 g of aggregates were gently
121 immersed into 95% ethanol solution for 10 min (Le Bissonnais, 1996) before being wet sieved for 10 min. Then, the amount of aggregates that had
122 resisted the sieving (WAS_{et}) and the percentage of aggregate loss ($Loss_{et}$) was determined according to the equations (2) and (3). The relative
123 percentage of slaking (RPS; Falsone and Bonifacio, 2006) was calculated as:

124 $$RPS = \frac{Loss - Loss_{et}}{Loss} \cdot 100 \quad (4)$$

125 The specific surface area was determined by N_2 gas adsorption at 77 K in the relative pressure (p/p°) range of 0.05-0.30 (Gregg and Sing, 1982) with
126 a Sorptomatic 1900 surface area analyser (CE instruments, Rodano, Italy) by applying the Brunauner-Emmett-Teller (BET) equation. Enough

127 sample was used for measurement to ensure a total surface area >10 m^2 (corresponding to around 1.2 g of sample). All samples were initially
128 degassed for 16 hours at 50°C. The micropore (<2 nm) volume and surface area were evaluated from the adsorption-desorption isotherms, using the
129 t-plot method (V_{MICRO} and S_{MICRO}, respectively; de Boer et al., 1966), while mesopores (2-50 nm; V_{MESO} and S_{MESO}) were derived from the
130 desorption branch according to Pierce's (1953) model.
131 Porosity characteristics were evaluated by Hg intrusion using a 2000 WS porosimeter equipped with a 120 Macropore unit (CE Instruments,
132 Rodano, Italy). The total volume of intruded Hg (i.e. total pore volume) was expressed on a mass basis (V_{TOT}, $mm^3\ g^{-1}$). The cumulative curve of
133 intruded Hg volume as a function of the pore radius was used to calculate the variation of the pore volume following Bruand and Prost (1987):

134 $$slope_{ij} = \frac{V_i - V_j}{\log_{10} R_j - \log_{10} R_i} \quad (5)$$

135 where the volumes *Vi* and *Vj* correspond to the radii *Ri* and *Rj* at two successive positions *i* and *j*. The values of the slope were then plotted against
136 the mean log radius, thus the relative maxima of the slope curve indicated the most represented classes of pores and corresponded to a modal radius
137 (expressed in μm). The volume of each modal class of pores was thus included between two minimum values of the slope, which defined the limits
138 of the class. This data treatment returns a bimodal distribution: two modal pore radii attributed to the packing of finer (clay) and coarser (sand and
139 silt) fractions, according to Fiès and Bruand, (1998). The corresponding volumes of pores were labelled as Vf and Vc. The modal pore size
140 corresponding to the coarser particles ranged between 0.152 to 1.565 μm, while the modal pore size corresponding to the finer particles ranged
141 between 0.005 and 0.022 μm (data not shown). The modal smaller pores were therefore in the range size of mesopores measured by N_2 adsorption
142 (Echeverría et al., 1999) and in this study we chose to use the N_2 adsorption data for finer pore size measurements.

The packing density of particles, i.e. the volume occupied by solid particles with respect to the total volume (space occupied by solid plus void space), was calculated according to Falsone and Bonifacio (2009) as:

$$packing\ density = \frac{particle\ mass}{particle\ density} \cdot \frac{1}{\frac{particle\ mass}{particle\ density} + volume\ of\ pores} \quad (6)$$

where particle density was taken equal to 2.65×10^{-3} g mm^{-3}, the mass was expressed in g (100 g)$^{-1}$, the volume of pores in mm^3 g^{-1}, and the resulting packing density was dimensionless. We calculated both the packing density of the sand-silt phase and of clay, using the particle size data obtained after dispersion of sample with $(NaPO_3)_6$ for particle mass, and the modal coarse volume (Vc) and the mesopores volume (V_{MESO}), respectively, for sand-silt and clay-clay interactions (Zong et al., 2015; Fiès and Bruand, 1998).

All the statistical analyses were carried out using SPSS 20 (SPSS Inc., Chicago, IL). Differences among samples were evaluated using the analysis of variance (ANOVA and Duncan's test). The threshold used for significance in all statistical tests was set at 0.05.

3. Results

3.1. 1-2 mm aggregates properties before treatments (without any treatment)

The 1-2 mm aggregate class of both fragipan (FRG) and non-fragipan (NFRG) horizons had low organic C content (<2 g kg^{-1}; Table 3). The content of pedogenic Fe oxides was high (Fe_{DCB}>60 g kg^{-1}; Table 3). FRG had high coarse sand content (CS: 49.4%; Table 3), while NFRG was rich in fine sand (FS: 44.4%; Table 3). The difference in coarse sand content among FRG and NFRG was also observed in the content of primary coarse sand-size particles (CS_{ox}: 7.4 and 24.9% for NFRG and FRG). The amount of clay was instead similar in the two horizons (10.7 and 13.0% for NFRG

and NFRG, respectively), as well as the clay dispersion ratio (CDR). The fragmentation behaviour in water of the 1-2 mm aggregate class of FRG showed a relative percentage of slaking of 30.1% (RPS; Table 4), giving a contribution to the wet-aggregate losses, as in general observed in fragipan horizons (Falsone et al., 2006). The N_2 adsorption at 77 K and Hg porosity data clearly evidenced the peculiarity of pores size distribution of FRG-aggregates: FRG had more mesopores than macropores (V_{MESO} and Vc, respectively, Figure 2A; Lamotte et al., 1997; Ajmone-Marsan et al., 1994), in opposition to NFRG. Because of high mesoporosity volume, the corresponding mesopores surface areas (S_{MESO}) were large in FRG (Figure 2B). The packing density of the coarser particles showed that typically FRG had a closer arrangement than NFRG (PDc: 0.82 and 0.73; Table 5). The packing density of the clay fraction showed instead a slightly more open arrangement in FRG than NFRG (PDf values: 0.31 and 0.39 for FRG and NFRG samples, Table 5). Before treatments, the 1-2 mm FRG aggregates had thus the highest PDc/PDf ratio (Table 5) as typical of fragipans i.e. an open packing of the clay phase associated to an extremely dense packing of sand and silt (Falsone and Bonifacio, 2009).

3.2. 1-2 mm aggregates properties after the wet-dry cycle

3.2.1. Fragipan

The amount of FRG aggregates maintaining the 1-2 mm size after one wet-dry cycle with deionized water was around 20% of the total mass (Figure 3A), while a lower percentage of 1-2 mm aggregates was obtained after $CaCl_2$ treatment (10.6%, Figure 3B). The clay fraction was the most affected by the presence of Ca, as expected, and the FRG-CA sample was enriched in flocculated clay with respected to both the untreated and water-treated samples (i.e. the CDR decreased, Table 3; $p<0.05$). The experiments destabilised all the treated-aggregates, as visible from the increase of the aggregate losses due to wet sieving (Loss and $Loss_{et}$ increased up to 68.8 g (100) g^{-1} in the case of FRG-CA, $p<0.05$; Table 4). The

losses due to slaking instead decreased (RPS, $p<0.05$; Table 4). Finally, also the pore system changed (Figure 2A): the treatments slightly increased the coarser pores volume (Vc) and reduced the mesopores volume (V_{MESO}). The volume of micropores also decreased following the Ca-treatment. As a result of the change in pore distribution, the finer particles in the treated-aggregates became more closely packed, especially in the Ca-treated sample, while the arrangement of coarser particles was slightly looser than those of untreated-FRG (PDf increased and PDc slightly decreased, respectively; Table 5), and the PDc/PDf ratio strongly decreased ($p<0.05$).

3.2.2. Non-fragipan

The amounts of NFRG aggregates that maintained the 1-2 mm size after wet-dry cycle with both deionized water and $CaCl_2$ were around 20% of the total mass (Figure 3A-B). Differently from FRG samples, the 1-2 mm aggregate class of NFRG samples had lower CS_{ox} content than the samples before the treatment (Table 3; $p<0.05$). The clay fraction appeared again more affected (Table 3): the NFRG-CA sample had higher clay content and lower clay dispersibility (i.e., lower CDR value; $p<0.05$) than NFRG before treatment, in contrast to NFRG-WAT that had similar clay content and higher dispersability (i.e., higher CDR value; $p<0.05$) than NFRG.

The treatments increased the aggregate losses by wet sieving (Loss and $Loss_{et}$, $p<0.05$: Table 4), but, after the Ca-treatment and differently from FRG sample, the losses due to slaking increased (i.e., RPS value increased, $p<0.05$; Table 4). As regards to the aggregate porosity, the mesopores volume and surface (V_{MESO} and S_{MESO}) increased after treatment (Figure 2A-B), while the volume and the surface of the micro (V_{MICRO} and S_{MICRO}) and the volume of coarser pores (Vc) decreased, especially after $CaCl_2$-treatment. As a result, the arrangement of finer particles appeared denser, while the packing density of coarser particles did not change with respect to those of NFRG (PDf increased and PDc did not vary, respectively;

194 Table 5). After the treatments, the packing density of the aggregates from NFRG and FRG became more similar than it was before, as visible also
195 by the PDc/PDf ratio (Table 5).
196
197 *3.3. NEW- aggregates properties obtained by wet-dry cycle*
198 *3.3.1. Fragipan*
199 After the treatment with deionized water, the 2-5 and >5 mm newly formed aggregates (FRG_{2-5}-WAT and FRG_5-WAT) composed 23.1 and 45.3%
200 of the total mass of FRG samples (Figure 3A), while after $CaCl_2$-treatment they represented 16.5 and 66.5%, (FRG_{2-5}-CA and FRG_5-CA; Figure
201 3B). The NEW-aggregate classes of FRG sample had low organic C content and high Fe_{DCB} amount (Table 6), as already observed for 1-2 mm
202 aggregates before and after treatments. The amount of coarse sand decreased in all NEW-aggregates with respect to the aggregates before treatments
203 ($p<0.05$; CS values in NEW-aggregates ranged from 29.2 to 40.1 g kg^{-1}, CS content was 49.4 g kg^{-1} in untreated-FRG aggregates; Table 6 and Table
204 3, respectively), as well as the content of primary coarse sand particles (CS_{ox}, $p<0.05$ Tables 3 and 6). As already observed for 1-2 mm aggregates,
205 after $CaCl_2$-treatment the clay content increased and this again corresponded to a slightly lower water dispersibility of the clay fraction, as CDR
206 decreased in NEW-aggregates after Ca-treatment ($p<0.05$; Table 6). In FRG the NEW-aggregates were extremely water fragile, and after wet
207 sieving their losses varied from 64.3 to 76.4% (Loss; Table 7). Similar values were found for $Loss_{et}$. However, the incidence of slaking on FRG
208 losses was extremely low, and for >5 mm NEW-aggregates the RPS values were even <2% (Table 7). The volume corresponding to the larger
209 pores, Vc, did not show any specific trend with the treatment (Figure 4A), as well as the PDc values (Table 8). However, the packing density of
210 coarser particles was lower than that of the FRG aggregates before treatments ($p<0.05$; for FRG, the PDc values in NEW-aggregates ranged from

211 0.70 to 0.78, while in 1-2 aggregates before treatments it was 0.82; Table 8 and 5, respectively). The FRG NEW-aggregate V_{MESO} ranged from 56.7
212 and 66.1 $mm^3 g^{-1}$ and S_{MESO} from 30.8 to 34.3 $m^2 g^{-1}$ (Figure 4A and B), thus a strong mesoporosity decline has occurred after treatments ($p<0.05$;
213 V_{MESO} and S_{MESO} of the 1-2 mm aggregates before treatments were 111.0 $mm^3 g^{-1}$ and 42.6 $m^2 g^{-1}$, Figure 2A-B). The Ca-treatment strongly affected
214 the microporosity, as visible from the very low volume and surface area of micropores in Ca-treated NEW-aggregates (Figure 4A-B). As a
215 consequence of the modification occurring in meso and microporosity, the PDf values increased in NEW-aggregates with respect to the 1-2 mm
216 aggregates before treatments ($p<0.05$; PDf values always ≥ 0.44 in NEW-aggregates vs. 0.31 in aggregates before treatments; Tables 8 and 5,
217 respectively), especially in the Ca-incubated samples.

218 *3.3.2. Non-fragipan*

219 After treatment of NFRG with deionized water, the 2-5 and >5 mm newly formed aggregates composed 25.0 and 20.1% of the total mass, while
220 after $CaCl_2$-treatment they represented 21.4 and 43.4%, respectively (Figure 3A-B). The organic C content was similar in all NFRG NEW-
221 aggregates (0.6-0.8 g kg^{-1}, Table 6), as well as the amount of pedogenic Fe oxides (50.5-53.0 g kg^{-1}, Table 6), even if the Fe_{DCB} content in NEW-
222 aggregates was lower than before treatments ($p<0.05$; Fe_{DCB} was 62.8 g kg^{-1} in the untreated-NFRG aggregates; Table 3). Similarly to the NEW-
223 aggregates of FRG, the coarse sand content decreased in the NEW-aggregates of NFRG with respect to the aggregates before treatments ($p<0.05$;
224 CS values in NF-aggregates ranged from 8.2 to 15.0 g kg^{-1}, CS content was 24.8 g kg^{-1} in untreated-NFRG aggregates; Table 6 and Table 3,
225 respectively), as well as the content of primary coarse sand particles ($p<0.05$; $CS_{ox;}$ Tables 3 and 6). The clay behaviour was similar to that of FRG
226 samples: the Ca-treated samples were enriched in flocculated clay (higher clay content and lower CDR values than water-treated samples; Table 6).
227 The NEW-aggregates were unstable to water stresses, and high losses of aggregates occurred (Loss and $Loss_{et}$ always >52%; Table 7), even if the

incidence of slaking was low (RPS always <13%; Table 7). The NFRG NEW-aggregates were still more stable than FRG ones but the differences were less marked. In the NFRG NEW-aggregates, the Vc values ranged from 97 to 123 mm^3 g^{-1} (Figure 4A) and the corresponding PDc varied from 0.73 to 0.76 (Table 8). Similar Vc and PDc values were thus found in both FRG and NFRG NEW-aggregates. No specific effect of the treatment conditions on the coarser porosity was found. Instead, similarly to FRG samples, the V_{MICRO} and S_{MICRO} strongly decreased after the Ca-treatment (Figure 4A-B). With respect to the sample before treatments, also in the case of NFRG NEW-aggregates, the PDf values increased especially in the Ca-incubated samples ($p<0.05$; PDf values varied from 0.42 to 0.54 in NEW-aggregates, and in aggregates before treatments PDf was 0.39; Tables 8 and 5, respectively).

4. Discussion

In this work, we wanted to evaluate the variations caused by a wet-dry cycle carried out in laboratory controlled conditions, using both deionized and Ca-enriched water on the 1-2 mm aggregate properties of a Btx horizon, and to investigate the physical properties of newly formed aggregates (i.e. 2-5 and >5 mm size classes) obtained after the experiment. This was performed in order to investigate the specific effect of alternating moisture conditions on the evolution of aggregates collected from Btx horizon. The same soil properties were monitored for the reference Bt horizon that did not show fragipan properties.

4.1. 1-2 mm aggregates properties of fragipan and non-fragipan before treatments

245 The characterisation of the 1-2 mm aggregates before the treatment experiments confirmed the typical physical properties of fragipans detectable in
246 laboratory and reported in Figure 6: high aggregate fragility against slaking (e.g., Soil Survey Staff, 2014; Falsone and Bonifacio, 2006; Lindbo and
247 Rhoton, 1996), low volume of macropores and high volume of micropores (e.g., Lamotte et al., 1997; Ajmone-Marsan et al., 1994), high density
248 (e.g., Falsone and Bonifacio, 2009; Weisenborn and Schaetzl, 2005b). Conversely, non-fragipan aggregates showed higher resistance to water-
249 breakdown and lower slaking susceptibility, had more macropores than micropores, and showed a more open arrangement of the coarse fraction
250 (Figure 6). The particle size distribution was however similar between the two horizons, and the low CDR values were in agreement with the
251 presence of flocculated clays in argillic horizons formed by lessivage (e.g., Schaetzl and Anderson 2005) and suggested a similar dispersion
252 behaviour of the clay fraction (Dong et al., 1983).
253
254 *4.2. Evolution of fragipan and non-fragipan 1-2 mm aggregates during laboratory controlled wet-dry cycle (deionized water and $CaCl_2$ effect)*
255 The wet-dry cycle affected the properties of the 1-2 mm aggregates from the fragipan, even if they maintained their size after the treatment and thus
256 did not take part in the formation of larger NEW-aggregates. Different effects of deionized and Ca-enriched water on aggregate dynamics were
257 observed. After treatment with deionized water, FRG 1-2 mm aggregates were enriched in easily dispersible clay (CDR values >20%; Table 3),
258 while the $CaCl_2$-treatment slightly increased the clay flocculation status (CDR values <10%). This means that, as expected, Ca addition enhanced
259 clay flocculation. In the presence of Ca^{2+} ions, the clay outer layer is thinner and electrostatic repulsion among clay particles is lower, allowing for
260 van der Waals' forces to promote the formation of small stacks of clay platelets (i.e., clay domains; Sposito, 1989). This arrangement favours face-
261 to-face association between clay particles (van Olphen, 1977), which might have caused the denser packing of the clay fraction indicated by the

increase of the PDf values. In contrast, water treatment had a lower effect on clay associations because clay arrangement was unaffected, as indicated by the similarity of PDf values between FRG treated and untreated 1-2 mm aggregates. As a result the PDc/PDf ratio, which can be used as a simple index of the combination of the coarser and finer particle density, decreased. Ramos et al. (2015) stated that the face-to-face association of kaolinite platelets favoured fragipan formation, but in our Ca-treated samples it causes the closure of clay packing minimising the differences between coarser and finer particle density. The aggregates after treatment did not thus show anymore the contrasting coarser-finer particles arrangement typical of fragipan (Falsone and Bonifacio, 2009). Moreover, the 1-2 mm aggregates of both treated-FRG were more water fragile after treatment, but they showed a higher relative resistance to slaking. It appeared therefore that the fragipan aggregates that did not take part in the formation of NEW-aggregates markedly lost the typical properties of fragipan investigated in this lab study (Figure 6).

4.3. Physical properties of newly-formed aggregates obtained from fragipan and non-fragipan horizons upon the laboratory wet-dry cycles (deionized water and $CaCl_2$ effect)

The formation of new aggregates in fragipan seems to have occurred through the interaction of clay floccules, and other soil coarse particles, likely sand grains and/or already existing aggregates, as indicated by clay quantity and quality in the NEW-aggregates. In fact, after both deionized water and $CaCl_2$ addition, the clay amount increased in FRG NEW-aggregates and its dispersibility decreased or was steady. The involvement of coarse particles, and thus the formation of aggregates due to clay floccules covering sand particles or already existing aggregates is in agreement with Falsone et al. (2007). They found that in the presence of poorly dispersible clay, the low electrostatic barrier allowed clay sized aggregates to form and subsequently cover sand grains during a wet-dry cycle with deionized water. Although in the present study we did not measure the surface

279 charge of clay fraction, both the low CDR values of the 1-2 mm aggregates before treatments and the selection of samples from argillic horizons
280 suggested a low surface charge of clay fraction. In these conditions, the addition of Ca^{2+} would further enhance clay flocculation, and the similarity
281 between samples (i.e., water and Ca-treated) in quantitative and qualitative clay data suggest the same pathway of aggregates formation in both
282 deionized water and $CaCl_2$ treated samples. The NEW-aggregates obtained after the treatments had a lower resistance to water stress than the
283 samples before treatments. This further confirmed the hypothesized aggregation pathway (i.e., clay-clay associations covering coarse particles), as
284 aggregate stability is lower when coarse particles are linked to an already flocculated clay phase (Attou et al., 1998; Falsone et al., 2007). As a
285 consequence of the new particle association, in FRG NEW-aggregates coarser particles had a more open arrangement (i.e., PDc values decreased).
286 The volume of mesopores instead decreased and, again, in the Ca-incubated samples the enhancement of clay flocculation affected the packing
287 density of clay with a closer arrangement after treatment (i.e., PDf values increased). In this study, the aggregates after treatments showed thus a
288 progressive decrease of PDc/PDf ratio. Considering the investigated physical parameters, it appeared therefore that also the FRG NEW-aggregates
289 did not show the typical properties of fragipan after both water and Ca-treatment (Figure 6).
290
291 *4.4. The overall experimental effect*
292 There was a general trend upon treatments that was independent from the type of horizon (FRG and NFRG) and the aggregate size (1-2 mm, 2-5
293 NF-aggregates, >5 mm NF-aggregates): the wet-dry cycle modified the spatial arrangements of both clay and coarser particles, with a denser
294 packing of the clay phase and an opening of the coarser particles arrangement. This was likely caused by the formation of face-to-face clay
295 associations and by associations between coarse particles and flocculated clays. The new particle arrangement worsened the aggregate water

resistance, and all the aggregates after treatments were indeed less water stable. However, our results suggested that this new particle arrangement contributed to limit the breakdown due to slaking, as the relative percentage of slaking decreased (r^2 always >0.5; Figure 5). This suggests that the opening of the coarse particles arrangement coupled to the closure of the clay particles packing limited aggregate breakdown due to slaking, thus further confirming that FRG samples obtained after treatments moved away from the typical physical behaviour of fragipans measureable in laboratory.

5. Conclusions

The water treatment promoted the enrichment in flocculated-clay in the NEW-aggregates, and Ca-treatment enhanced clay flocculation both in the NEW- and in the 1-2 mm aggregates that maintained their size. However, the hypothesized enhancement of fragipan properties (such as slaking, particle density and porosity), due to the increase in clay flocculation did not take place in our samples. The clay flocculation in fact induced a denser arrangement of clay particles, and a consequent reduction of mesopores, combined with the opening of the coarser particles packing. This new particle arrangement did not correspond to the specific combination of coarse/fine particles arrangement of fragipans detectable in laboratory conditions. These results point to the importance of the clay fraction, and particularly of the dispersible clay fraction, but more research is needed to understand its role in driving argillic Bx properties.

6. References

313 Ajmone-Marsan, F., Pagliai, M., Pini, R., 1994. Identification and properties of fragipan soils in the Piemonte Region of Italy. Soil Sci. Soc. Am. J.
314 58, 891-900.
315 Attou, F., Bruand, A. , Le Bissonnais, Y., 1998. Effect of clay content and silt-clay fabric on stability of artificial aggregates. Eur. J. Soil Sci.
316 49:569–577.
317 Attou, F., Bruand, A., 1998. Experimental study of 'fragipans' formation in soils. Role of both clay dispersion and wetting-drying cycles. C. R.
318 Acad. Sci. 326, 545–552. DOI: 10.1016/S1251-8050(98)80205-X
319 Bockheim, J.G., Hartemink, A.E., 2013. Soils with fragipans in the USA. Catena 104, 233–242. DOI: 10.1016/j.catena.2012.11.014
320 Boulet, R., Fritsch, E., Filizola, H.F., de Araujo Filho, J.C., Leprun, J.C., Barretto, F., Balan, E., Tessier, D., 1998. Iron bands, fragipans and
321 duripans in the northeastern plateaus of Brazil – properties and genesis. Can. J. Soil Sci. 78, 519-530.
322 Bruand, A., Prost, R., 1987. Effect of water content on the fabric of soil material: an experimental approach. J. Soil Sci. 38, 461–472.
323 Bruckert, S., Bekkary, M., 1992. Effect of rock permeability on the formation of diagnostic argillic and fragipan horizons. Can. J. Soil Sci. 72, 69-
324 88.
325 De Boer, J.H., Lippens, B.C., Linsen, B.G., Broekhoff, J.C.P., van den Heuval, A., Osinga T.J., 1966. The t-curve of multimolecular N_2-adsorption.
326 J. Colloid. Interf. Sci. 21, 405-414.
327 Dong, A., Chesters, A., Simsinan, G.V., 1983. Soil dispersibility. Soil Sci. 136, 208-212.
328 Echeverría, J.C., Morera, M.T., Mazkiarán, C., Garrido, J.J., 1999. Characterization of the porous structure of soils: adsorption of nitrogen (77K)
329 and carbon dioxide (273K), and mercury porosimetry. Eur. J. Soil Sci. 50, 497-503. DOI: 10.1046/j.1365-2389.1999.00261.x

330 Falsone, G., Bonifacio, E., 2006. Destabilization of aggregates in some Typic Fragiudalfs. Soil Sci. 171, 272-281. DOI:
331 10.1097/01.ss.0000199703.76278.80
332 Falsone, G., Bonifacio, E., 2009. Pore-size distribution and particle arrangement in fragipan and non fragipan horizons. J. Plant Nutr. Soil Sci. 172,
333 696-703. DOI: 10.1002/jpln.200800066
334 Falsone, G., Celi, L., Bonifacio, E., 2007. Aggregate formation in chloritic and serpentinitic alpine soils. Soil Sci. 12, 1019-1030. DOI:
335 10.1097/ss.0b013e31815778a0

336 Falsone, G., Celi, L., Stanchi, S., Bonifacio, E., 2016. Relative importance of mineralogy and organic matter characteristics on macroaggregate and
337 colloid dynamics in Mg-silicate dominated soils. Land Degrad. Develop. 27, 1700-1708. DOI: 10.1002/ldr.2516

338 Fiès, J. C., Bruand, A., 1998. Particle packing and organization of the textural porosity in clay-silt-sand mixtures. Eur. J. Soil Sci. 49, 557–567.
339 Forno, G.M., Gregorio, L., Vatteroni, R., 2007. La successione stratigrafica del settore destro del Conoide di Lanzo e il suo significato per l'utilizzo
340 del territorio. Mem. Soc. Geogr. It. 87, 237-247.
341 Gee, G. W., Bauder, J. W., 1986. Particle-size analysis, in: Klute, A.(Ed.), Methods of soil analysis, Part 1. 2nd edn., Agron. Monogr. No. 9, ASA
342 and SSSA, Madison, Wisconsin, USA, pp. 383–411.

343 Fortun, A., C. Fortun, and C. Ortega. 1989. Effect of farmyard manure and its humic fractions on the aggregate stability of a sandy-loam soil. J. Soil
344 Sci. 40, 293–298.

345 Gregg, S.J., Sing, K.S.W., 1982. Adsorption surface area and porosity. 2nd edition. Academic Press. London, UK.

346 Kemper, W.D., Rosenau, R.C., 1984. Soil cohesion as affected by time and water content. Soil Sci. Soc. Am. J. 48, 1001-1006.

347 Lamotte, M., Bruand, A., Humbel, F. X., Herbillon, A. J., Rieu, M., 1997. A hard sandy-loam soil from semi-arid Northern Cameroon: I. Fabric of
348 the groundmass. Eur. J. Soil Sci. 48, 213–225.

349 Le Bissonnais, Y., 1996. Aggregate stability and assessment of soil crustability and erodibility: I. Theory and methodology. Eur. J. Soil. Sci. 47,
350 425-437.

351 Lindbo, D.L., Rhoton, F.E., 1996. Slaking in fragipan and argillic horizons. Soil Sci. Soc. Am. J. 60, 552-554.

352 Lindbo, D.L., Rhoton, F.E., Bigham, J.M., Hudnall, W.H., Jones, F.S., Smeck, N.E., Tyler, D.D., 1994. Bulk-density and fragipan identification in
353 loess soils of the Lower Mississipi River Valley. Soil Sci. Soc. Am. J. 59, 487-500.

354 Mehra, O. P., Jackson, A., 1960. Iron oxide removal from soils and clays by a dithionite citrate system buffered with sodium bicarbonate, in:
355 Proceedings of 7th National Conference of clay and minerals. Washington, DC. 1958. Pergamon Press, New York city, New York, pp. 317-327.

356 Nikorych, V.A., Szymański, W., Polchyna, S.M., Skiba, M., 2014. Genesis and evolution of the fragipan in Albeluvisols in the Precarpathias in
357 Ukraine. Catena 119, 154-165. DOI: 10.1016/j.catena.2014.02.011

358 Pierce, C., 1953. Computation of pore size from physical adsorption data. J. Phys. Chem. 57, 149-152.

359 Ramos, M.R., Melo V.F., Uhlmann, A., Dedecek R.A., Curcio G.R., 2015. Clay mineralogy and genesis of fragipan in soils from Southeast Brazil.
360 Catena 135, 22-28. DOI: 10.1016/j.catena.2015.06.016

Schaetzl, R.J., Anderson, S., 2005. Soils: Genesis and Geomorphology. Cambridge University Press, NY, USA.

Schoeneberger, P.J., Wysocki, D.A., Benham, E.C., Soil Survey Staff, 2012. Field book for describing and sampling soils. Version 3.0. Natural Resources Conservation Service. National Soil Survey Center, Lincoln, NE.

Soil Survey Staff. 2014. Keys to soil taxonomy, 12th edn. USDA-Natural Resources Conservation Service, Washington, DC.

Sposito, G., 1989. The chemistry of soils. Oxford University Press, New York City, New York.

Stanchi, S., Catoni, M., D'Amico, M.E., Falsone, G., Bonifacio, E. 2017. Liquid and plastic limits of clayey, organic C-rich mountain soils: role of organic matter and mineralogy. Catena 151, 238-246. DOI: 10.1016/j.catena.2016.12.021

Szymański, W., Skiba, M., Skiba, S., 2011. Fragipan horizon degradation and bleached tongues formation in Albeluvisols of the Carpathian Foothills, Poland. Geoderma 167–168, 340–350. DOI: 10.1016/j.geoderma.2011.07.007

van Olphen, H., 1977. An introduction to clay colloid chemistry. J. Wiley & Sons, New York City, New York.

Weisenborn, B.N., Schaetzl, R.J., 2005a. Range of fragipan expression in some Michigan soils: II. A model for fragipan evolution. Soil Sci. Soc. Am. J. 69, 178–187.

Weisenborn, B.N., Schaetzl, R.J., 2005b. Range of fragipan expression in some Michigan soils: I. Morphological, micromorphological, and pedogenic characterization. Soil Sci. Soc. Am. J. 69, 168–177.

Wilson, M.A., Indorante, S.J., Lee, B.D., Follmer, L., Williams, D.R., Fitch, B.C., McCauley, W.M., Bathgate, J.D., Grimley, D.A., Kleinschmidt, K., 2010. Location and expression of fragic soil properties in a loess-covered landscape, southern Illinois, USA. Geoderma 154, 529–543. DOI: 10.1016/j.geoderma.2009.03.003

Zong, Y., Yu, X., Zhu, M., Lu, S., 2015. Characterizing soil pore structure using nitrogen adsorption, mercury intrusion porosimetry, and synchrotron-radiation-based X-ray computed microtomography techniques. J. Soil. Sediment. 15, 302-312. DOI: 10.1007/s11368-014-0995-0

Figure Captions

Figure 1. Scheme of the experiment.

Figure 2. Porosity (A) and surface area (B) of 1-2 mm aggregates of Btcx and Btc2 soil horizon before treatments (horizon code: FRG and NFRG) and after treatments (horizon code: FRG-WAT, FRG-CA, NFRG-WAT, NFRG-CA). The numbers inside the graphs are the absolute values of pore volume ($mm^3\ g^{-1}$) and surface area ($m^2\ g^{-1}$).

Figure 3. Percentage distribution of aggregates classes obtained after wet-dry cycle with A) deionized water and B) 0.25M $CaCl_2$.

Figure 4. Porosity (A) and surface area (B) of newly formed 2-5 and >5 mm aggregate of FRG and NFRG (Btcx and Btc2 soil horizon) obtained after treatments (horizon code: FRG-WAT, FRG-CA, NFRG-WAT, NFRG-CA). The numbers inside the graphs are the absolute values of pore volume ($mm^3\ g^{-1}$) and surface area ($m^2\ g^{-1}$).

Figure 5. Relationships between particle density of coarse particle-to-particle density of fine particles (PDc/PDf) ratio and relative percentage of slaking (RPS) in the samples obtained after wet-dry cycles with A) deionized water (r^2=0.671; p=0.013) and B) 0.25M $CaCl_2$ (r^2=0.514; p=0.045). Both in the upper and lower figure the 1-2 mm aggregates of Bx and Bt before treatments ($FRG_{before\ treatment}$ and $NFRG_{before\ treatment}$, respectively) are also reported.

Figure 6. Qualitative evolution of fragipan properties upon wetting and drying in lab conditions, depicted on an arbitrary scale (from 1 to 5) after A) deionized water cycle and B) $CaCl_2$-treatment in the different aggregate classes compared to soil fragipan and non-fragipan before treatments. The investigated fragipan properties are slaking (Soil Survey Staff, 2014; Falsone and Bonifacio, 2006; Lindbo and Rhoton, 1996), macroporosity (Lamotte et al., 1997; Ajmone-Marsan et al., 1994), particle density (Falsone and Bonifacio, 2009; Weisenborn and Schaetzl, 2005b) and microporosity (Lamotte et al., 1997; Ajmone-Marsan et al., 1994) measured in this study by high values of RPS values, low amount of Vc, high values of PDc and high amount of V_{MESO}, respectively. The highest is the rank, the best expressed the property. Note that in B) there are overlapping lines for FRG-CA and $FRG_{2\text{-}5}$-CA samples.

Tables

Table 1. Main morphological properties of the soil profile. Codes according to Schoeneberger et al. (2012)

Horizons	depth	Boundary	Munsell colour (dry)	Mottles	Structure	Coatings	Concentration	Rock fragments	Roots
	cm	D_T	Q_S_C	colour	G_S_T	Q_K	Q_S_K	volume%	Q_S

Oi	1-0	A_S	-	-	-	-	-	-	-	-
A	0-10	A_S	2.5Y6/4	-	-	2_f_gr		-	1	3_f
Bwc1	10-30	A_W	2.5Y6/6	f_1_d	2.5Y2.5/1	3_m_abk		1_2_FMN	5	3_f
Bwc2	30-60	C_W	2.5Y7/4	c_2_p	2.5Y2.5/1; 7.5YR6/8; 10YR6/8	3_m_abk		2_2_FMN	5	2_f
Btc1	60-120	C_W	10YR7/4	c_2_d	2.5Y5/1; 10YR4/3; 10YR6/8	3_co_abk	1_c	2_2_FMN	5	2_f
Btc2	120-165	A_S	10YR7/6	c_2_d	2.5Y2.5/1; 5YR4/6; 5YR4/3	2_co_abk	2_c	2_2_FMN	5	0
Btcx	165-190	A_S	7.5YR4/6	c_3_d	2.5Y2.5/1; 7.5YR6/8; 10YR7/6	3_co_pr	2_c	2_2_FMN	5	0
BC	190-245	C_W	5YR4/6	c_3_d	5YR2.5/1	3_co_abk	1_c	-	30	0
C	245-300	G_B	10YR4/6	c_3_d	5YR2.5/1; 5YR4/6; 10YR6/2	2_co_abk	-	-	70	0

Horizon boundary: (D) Distinctness: A=abrupt, C=clear, G=gradual; (T) Topography: S=smooth, W=wavy, U=unknown

Mottles: (Q) Quantity: f=few, c=common; (S) Size class: 1=fine, 2=medium; 3=coarse; (C) Contrast: d=distinct, p=prominent

Texture: SCL=sandy clay loam, SL=sandy loam. L=loam, C=clay

Structure: (G) Grade: 2=moderate, 3=strong; (S) Size class: f=fine, m=medium, co=coarse; (T) Type: gr=granular, abk= angular blocky, pr=prismatic

Coatings: (Q) Quantity: 1=few, 2=common; (K) Kind: c= clay

Concentrations: (Q) Quantity: 1=few, 2=common, 3=many; (S) Size class: 3=coarse; (K) Kind: FMN= iron-manganese masses

Roots: (Q) Quantity: 0=absent/very few, 1=few, 3=many; (S) Size class: f=fine

Table 2. Main properties of the <2 mm fraction of the selected Btc2 and Btcx soil horizons

Horizon	pH	Organic C	CS	FS	S	C	Fe_{DCB}	Ca saturation	Total porosity	V_{TOT}	SSA	Clay mineralogy

		g kg^{-1}	g kg^{-1}	g kg^{-1}	g kg^{-1}	g kg^{-1}	g kg^{-1}	%	%	mm^3 g^{-1}	m^2 g^{-1}	
Btc2	6.1	1.2	57.7	29.5	29.5	12.7	56.0	27.6	40	265	34.5	HIV (44%), Sm (28%), IV (15%), I (13%)
Btcx	6.1	2.2	59.5	26.2	26.2	14.2	77.3	21.3	38	240	48.4	HIV (37%), Sm (34%), IV (15%), I (14%)

CS: coarse sand (2-0.2 mm); FS: fine sand (0.2-0.05 mm); S: silt (0.05-0.002 mm); C: clay (<2 μm); Ca saturation: percentage of exchangeable Ca/cation exchange capacity; V_{TOT}: total volume of Hg intruded; SSA: specific surface area; Clay mineralogy was evaluated by X-ray diffraction (Co-Kα radiation) on Mg-saturated, ethylene glycol solvated and 550°C-heated oriented clay fraction-mounts - scans were made from 3 to 35°2θ at a speed of 1.5°2θ min-1 and a semi-quantitative evaluation of mineral abundance was performed as described in Stanchi et al. (2017): HIV, hydroxy-interlayered vermiculite; Sm, smectite; IV, randomly interstratified illite-vermiculite mixed layers; I, illite; numbers inside brackets are the relative abundance

427 Table 3. Organic C, pedogenic Fe oxides and particle size distribution of the 1-2 mm aggregate

428 class of FRG and NFRG (Btcx and Btc2 soil horizon) before treatments and after the wet-dry cycle.

sample code	treatment	Organic C	Fe_{DCB}	Particle size distribution after dispersion with $(NaPO_3)_6$				CS_{ox}	CDR
				CS	FS	S	C		
		g kg^{-1}	g kg^{-1}	%				g kg^{-1}	%
FRG	before treatments (without any treatment)	1.9±0.1	86.8±3.2	49.4±2.4	17.4±1.2	20.1±0.8	13.0±0.4	24.9±0.7	11.5±0.2
FRG-WAT	water treatment	1.7±0.2	88.3±1.1	51.0±0.1	16.2±0.1	23.2±3.0	9.6±3.2	33.0±0.4	20.8±4.3
FRG-CA	$CaCl_2$-treatment	1.4±0.2	94.8±3.9	39.1±0.7	16.6±0.7	25.5±0.2	18.7±0.2	31.5±3.3	9.1±0.8
NFRG	before treatments (without any treatment)	1.3±0.1	62.8±1.8	24.8±5.4	44.4±8.8	20.1±3.3	10.7±0.1	7.4±0.5	12.1±1.8
NFRG-WAT	water treatment	1.1±0.2	61.5±2.8	20.5±0.3	37.2±7.6	32.0±2.4	10.4±4.9	4.1±0.2	25.0±3.2
NFRG-CA	$CaCl_2$-treatment	0.9±0.3	53.5±0.7	15.6±3.1	30.2±2.9	34.5±0.8	19.6±0.5	4.4±0.5	9.2±1.4

429 CS: coarse sand (2-0.2 mm); FS: fine sand (0.2-0.05 mm); S: silt (0.05-0.002 mm); C: clay (<2 µm); CS_{ox}:

430 coarse sand obtained after H_2O oxidation and Na-dithionite-citrate-bicarbonate extraction followed by

431 $(NaPO_3)_6$ dispersion; CDR: clay dispersion ratio

432

433 Table 4. Wet stability of the 1-2 mm aggregate class of Btcx and Btc2 soil horizon before

434 treatments (horizon codes: FRG and NFRG) and after the wet-dry cycle.

sample code	treatment	Loss	$Loss_{et}$	RPS
		%	%	%
FRG	before treatments (without any treatment)	30.2±1.1	21.1±0.5	30.1±0.9
FRG-WAT	water treatment	58.1±0.2	44.5±4.1	23.4±4.2
FRG-CA	$CaCl_2$-treatment	68.8±3.6	58.5±2.9	15.0±8.7
NFRG	before treatments (without any treatment)	20.7±2.5	16.2±1.2	21.7±2.4
NFRG-WAT	water treatment	41.7±1.7	34.8±2.7	16.5±3.0
NFRG-CA	$CaCl_2$-treatment	44.7±1.0	32.6±0.5	27.1±1.8

435 Loss: percentage of aggregates lost after 10 min of wet sieving; $Loss_{et}$: percentage of aggregates

436 lost after pre-wetting in ethanol and 10 min of wet sieving; RPS: relative percentage of slaking

437

438

439 Table 5. Packing density of coarser (sand and silt) and finer (clay) particles (PDc and PDf,
440 respectively) of the 1-2 mm aggregate class of Btcx and Btc2 soil horizons before treatments
441 (horizon codes: FRG and NFRG) and after the wet-dry cycle.

sample code	treatment	PDc	PDf	PDc/PDf
FRG	before treatments (without any treatment)	0.82±0.01	0.31±0.01	2.65±0.06
FRG-WAT	water treatment	0.79±0.01	0.39±0.08	2.02±0.16
FRG-CA	$CaCl_2$-treatment	0.79±0.01	0.54±0.01	1.47±0.01
NFRG	before treatments (without any treatment)	0.73±0.01	0.39±0.01	1.87±0.02
NFRG-WAT	water treatment	0.73±0.01	0.34±0.10	2.16±0.06
NFRG-CA	$CaCl_2$-treatment	0.74±0.01	0.53±0.01	1.39±0.02

442

443 Table 6. Organic C, pedogenic Fe oxides and particle size distribution of newly formed 2-5 and >5 mm aggregates of FRG and NFRG (Btcx and

444 Btc2 soil horizons) obtained after the wet-dry cycle.

NF-aggregate class	sample code	treatment	Organic C	Fe_{DCB}	Particle size distribution after dispersion with $(NaPO_3)_6$				CS_{ox}	CDR
					CS	FS	S	C		
			g kg^{-1}	g kg^{-1}	g kg^{-1}				g kg^{-1}	%
2-5 mm	FRG_{2-5}-WAT	water treatment	1.5±0.1	95.5±0.7	40.1±0.5	24.3±5.1	22.5±4.7	13.0±0.1	24.9±1.3	9.2±2.1
	FRG_{2-5}-CA	$CaCl_2$-treatment	1.0±0.1	73.3±0.4	31.7±1.4	21.3±1.0	26.6±2.3	20.4±0.1	22.2±1.2	8.8±1.5
>5 mm	FRG_5-WAT	water treatment	1.3±0.1	80.5±0.1	36.2±0.6	29.2±4.9	20.7±2.3	13.9±2.0	17.3±0.1	13.7±2.2
	FRG_5-CA	$CaCl_2$-treatment	1.2±0.2	74.3±2.5	29.2±0.7	20.9±5.9	27.3±4.5	22.6±2.1	17.9±1.0	8.4±1.7
2-5 mm	$NFRG_{2-5}$-WAT	water treatment	0.7±0.1	50.8±1.1	14.8±0.2	33.9±0.9	37.8±0.1	13.5±0.8	4.1±0.8	16.3±1.4
	$NFRG_{2-5}$-CA	$CaCl_2$-treatment	0.8±0.2	51.8±0.4	10.8±1.2	35.1±3.1	35.4±1.8	18.8±0.1	3.9±0.3	10.1±0.7
>5 mm	$NFRG_5$-WAT	water treatment	0.6±0.1	53.0±0.1	15.0±0.4	34.8±4.9	36.5±3.2	13.8±1.4	3.2±0.6	17.2±3.2
	$NFRG_5$-CA	$CaCl_2$-treatment	0.6±0.1	50.5±0.2	8.2±1.5	33.3±3.9	38.6±2.2	19.9±0.2	4.0±0.4	11.1±1.8

445 CS: coarse sand (2-0.2 mm); FS: fine sand (0.2-0.05 mm); S: silt (0.05-0.002 mm); C: clay (<2 µm); CS_{ox}: coarse sand obtained after H_2O oxidation and

446 Na-dithionite-citrate-bicarbonate extraction followed by $(NaPO_3)_6$ dispersion; CDR: clay dispersion ratio

447

448 Table 7. Wet stability of newly formed 2-5 and >5 mm aggregates of FRG and NFRG (Btcx and
449 Btc2 soil horizons) obtained after the wet-dry cycle.

NF-aggregate class	sample code	treatment	Loss	$Loss_{et}$	RPS
			%	%	%
2-5 mm	FRG_{2-5}-WAT	water treatment	66.1±0.8	63.2±1.6	4.4±1.1
	FRG_{2-5}-CA	$CaCl_2$-treatment	76.4±2.0	67.8±0.7	11.2±1.4
>5 mm	FRG_5-WAT	water treatment	64.3±0.1	63.2±3.9	1.8±5.9
	FRG_5-CA	$CaCl_2$-treatment	76.1±1.9	75.1±1.4	1.3±0.6
2-5 mm	$NFRG_{2-5}$-WAT	water treatment	57.2±1.0	52.2±0.6	8.7±2.6
	$NFRG_{2-5}$-CA	$CaCl_2$-treatment	60.3±0.6	53.9±1.1	10.7±2.7
>5 mm	$NFRG_5$-WAT	water treatment	58.4±0.5	58.4±0.1	0.1±0.8
	$NFRG_5$-CA	$CaCl_2$-treatment	65.3±0.8	57.2±1.5	12.5±1.3

450 Loss: percentage of aggregate lost after 10 min of wet sieving; $Loss_{et}$: percentage of aggregate lost
451 after pre-wetting in ethanol and 10 min of wet sieving; RPS: relative percentage of slaking

452

453 Table 8. Packing density of coarser (sand and silt) and finer (clay) particles (PDc and PDf,
454 respectively) of newly formed 2-5 and >5 mm aggregates of FRG and NFRG (Btcx and Btc2 soil
455 horizons) obtained after treatments.

NEW-aggregate class	sample code	treatment	PDc	PDf	PDc/PDf
2-5 mm	FRG_{2-5}-WAT	water treatment	0.75±0.01	0.47±0.01	1.60±0.01
	FRG_{2-5}-CA	$CaCl_2$-treatment	0.78±0.01	0.58±0.01	1.34±0.01
>5 mm	FRG_5-WAT	water treatment	0.77±0.01	0.44±0.03	1.75±0.14
	FRG_5-CA	$CaCl_2$-treatment	0.70±0.01	0.59±0.02	1.19±0.05
2-5 mm	$NFRG_{2-5}$-WAT	water treatment	0.73±0.01	0.43±0.02	1.70±0.06
	$NFRG_{2-5}$-CA	$CaCl_2$-treatment	0.76±0.01	0.48±0.01	1.58±0.01
>5 mm	$NFRG_5$-WAT	water treatment	0.73±0.01	0.42±0.02	1.74±0.10
	$NFRG_5$-CA	$CaCl_2$-treatment	0.75±0.01	0.54±0.01	1.39±0.01

456

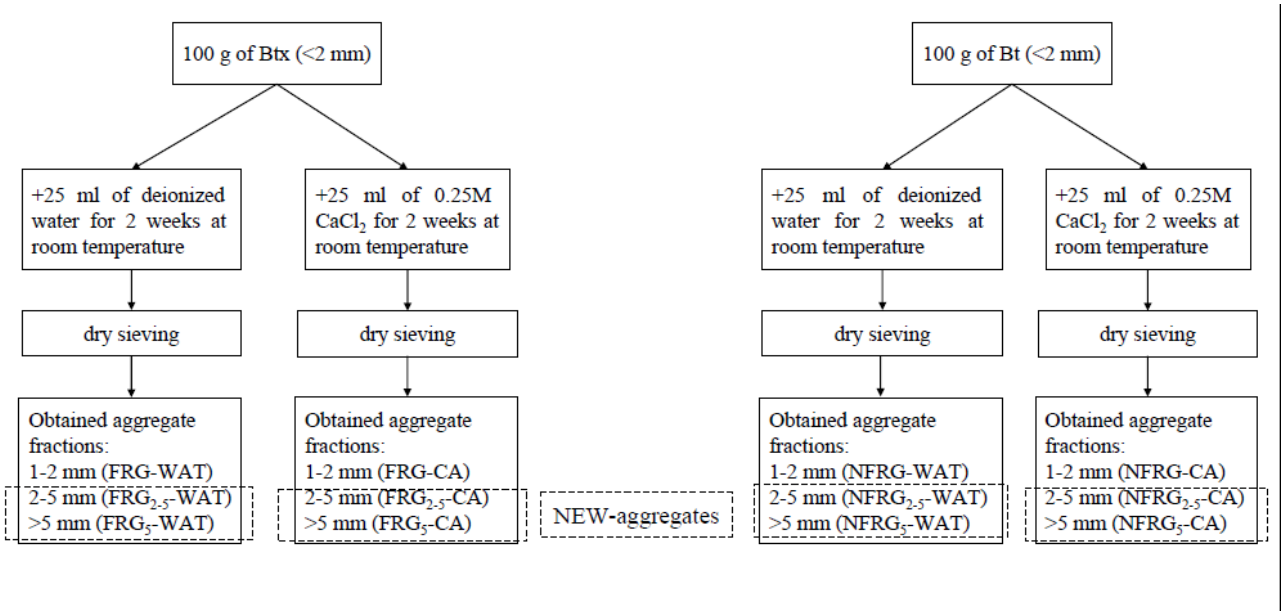

457

458

459

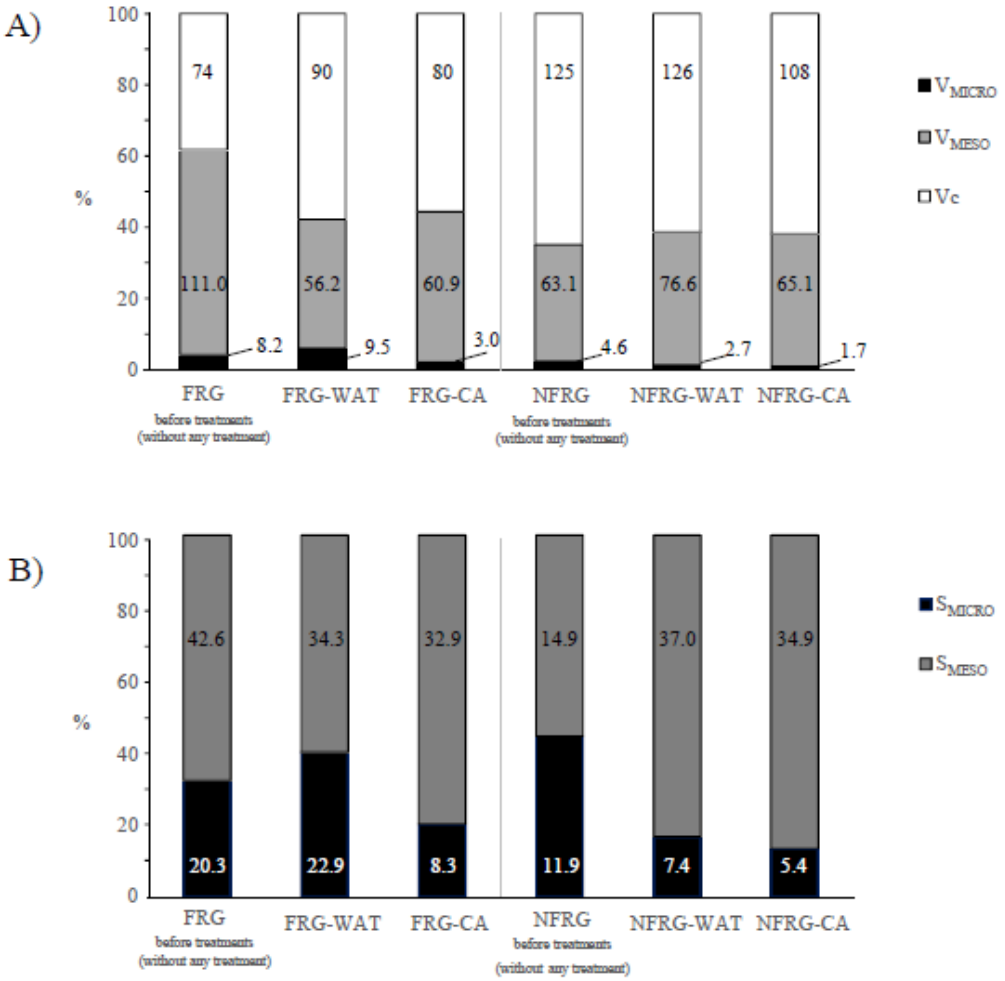
A)
100
80
60
40
20
0
%
74
90
80
125
126
108
111.0
56.2
60.9
63.1
76.6
65.1
8.2
9.5
3.0
4.6
2.7
1.7
FRG
before treatments
(without any treatment)
FRG-WAT
FRG-CA
NFRG
before treatments
(without any treatment)
NFRG-WAT
NFRG-CA
V_{MICRO}
V_{MESO}
Vc
B)
100
80
60
40
20
0
%
42.6
34.3
32.9
14.9
37.0
34.9
20.3
22.9
8.3
11.9
7.4
5.4
FRG
before treatments
(without any treatment)
FRG-WAT
FRG-CA
NFRG
before treatments
(without any treatment)
NFRG-WAT
NFRG-CA
S_{MICRO}
S_{MESO}

460

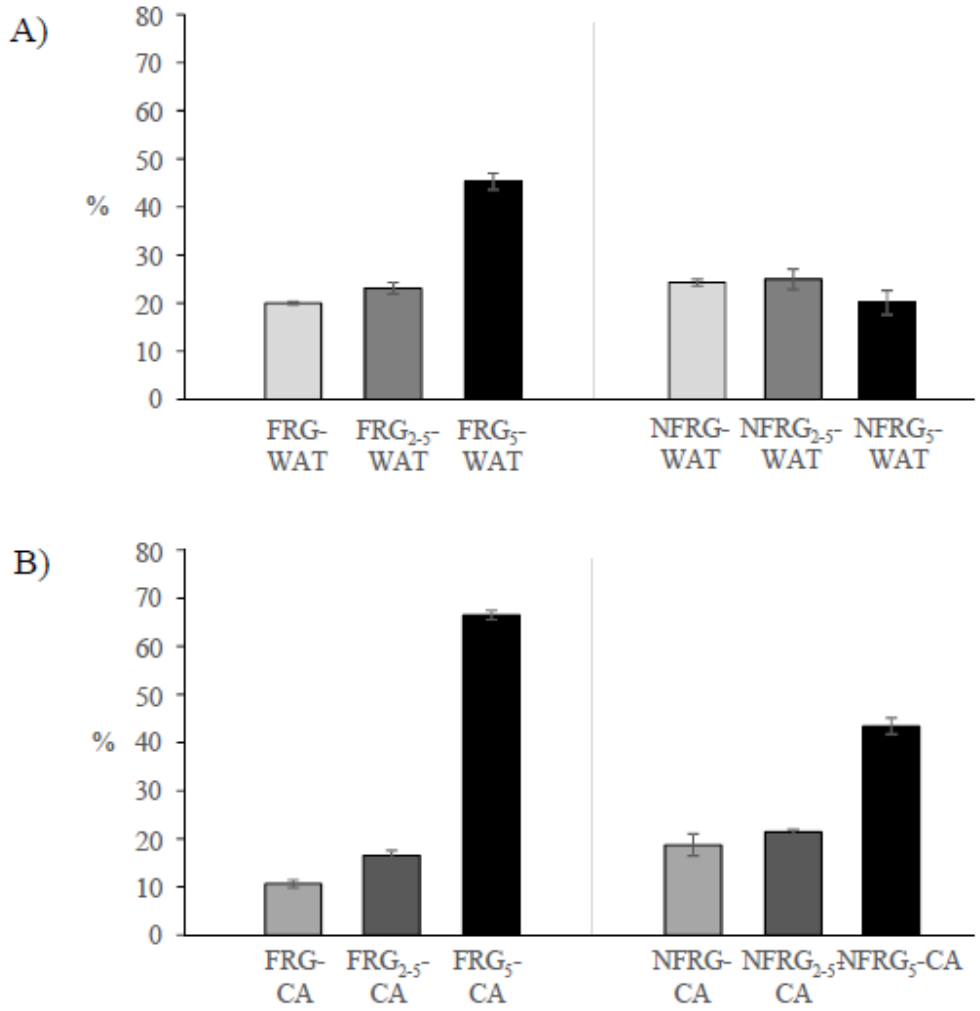
A)
80
70
60
50
%
40
30
20
10
0
FRG-WAT
FRG2-5-WAT
FRG5-WAT
NFRG-WAT
NFRG2-5-WAT
NFRG5-WAT
B)
80
70
60
50
%
40
30
20
10
0
FRG-CA
FRG2-5-CA
FRG5-CA
NFRG-CA
NFRG2-5-CA
NFRG5-CA

461

A)

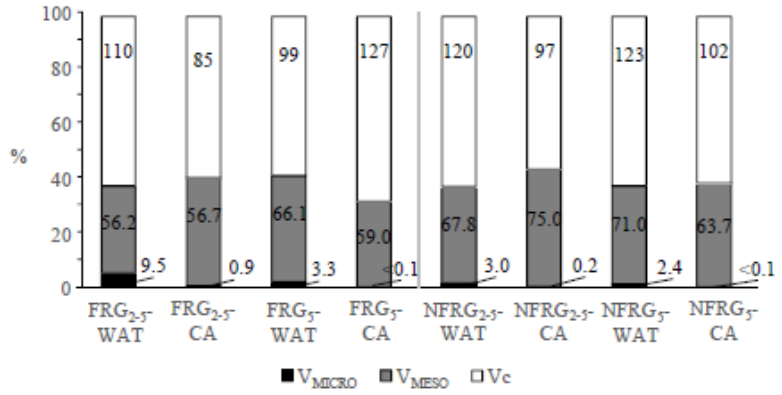
100
80
60
40
20
0
%
110
85
99
127
120
97
123
102
56.2
56.7
66.1
59.0
67.8
75.0
71.0
63.7
9.5
0.9
3.3
<0.1
3.0
0.2
2.4
<0.1
FRG2-5-WAT
FRG2-5-CA
FRG5-WAT
FRG5-CA
NFRG2-5-WAT
NFRG2-5-CA
NFRG5-WAT
NFRG5-CA
VMICRO
VMESO
Vc

B)

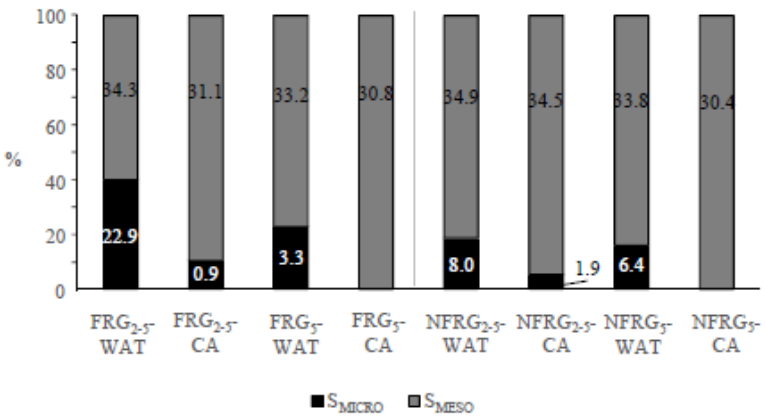
100
80
60
40
20
0
%
34.3
31.1
33.2
30.8
34.9
34.5
33.8
30.4
22.9
0.9
3.3
8.0
1.9
6.4
FRG2-5-WAT
FRG2-5-CA
FRG5-WAT
FRG5-CA
NFRG2-5-WAT
NFRG2-5-CA
NFRG5-WAT
NFRG5-CA
SMICRO
SMESO

462

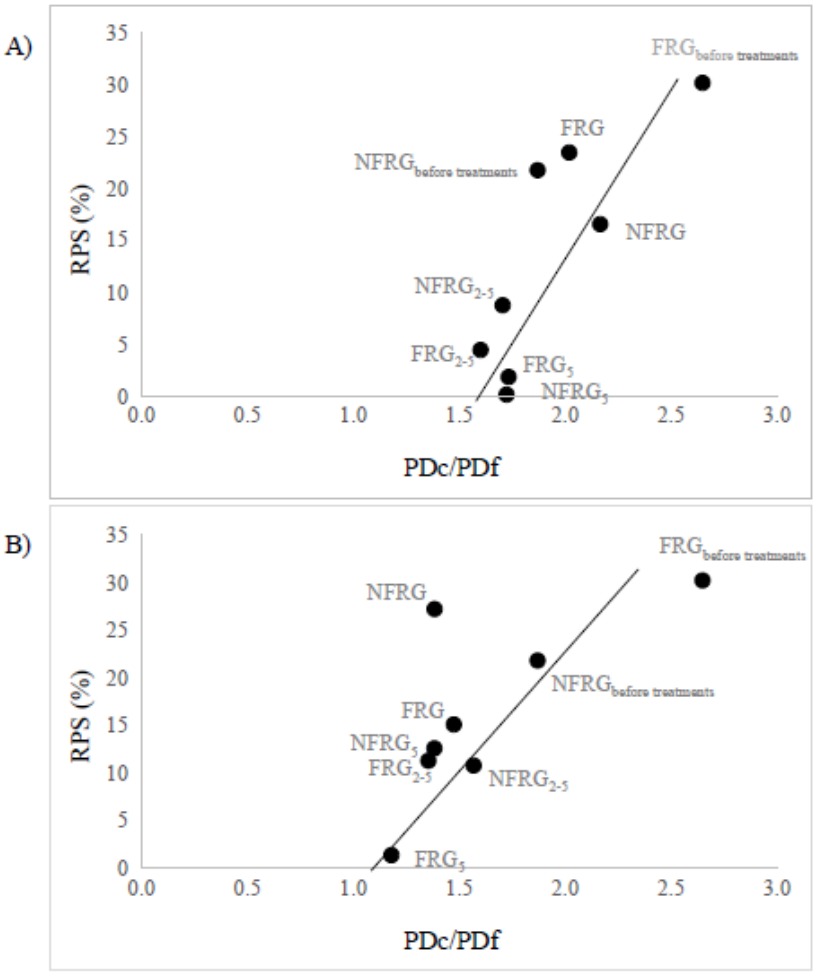
A)
RPS (%)
PDc/PDf
FRG before treatments
FRG
NFRG before treatments
NFRG
NFRG2-5
FRG2-5
FRG5
NFRG5
B)
RPS (%)
PDc/PDf
FRG before treatments
NFRG
NFRG before treatments
FRG
NFRG5
FRG2-5
NFRG2-5
FRG5

463

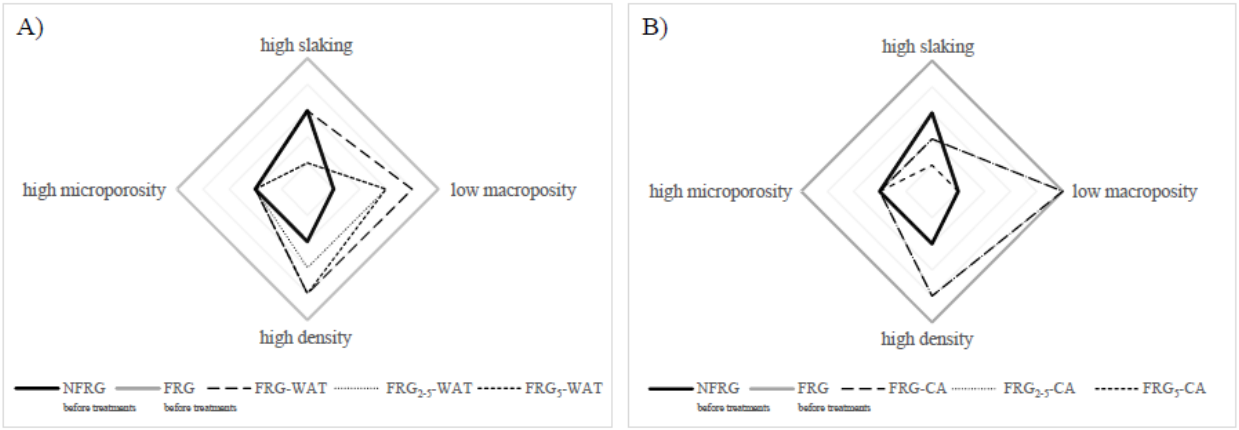
A)
high slaking
high microporosity
low macroporosity
high density
NFRG before treatments
FRG before treatments
FRG-WAT
FRG2-5-WAT
FRG5-WAT
B)
high slaking
high microporosity
low macroporosity
high density
NFRG before treatments
FRG before treatments
FRG-CA
FRG2-5-CA
FRG5-CA

464